Med Oncol (2017) 34:6
DOI 10.1007/s12032-016-0862-5

ORIGINAL PAPER

K-Ras, H-Ras, N-Ras and B-Raf mutation and expression analysis in Wilms tumors: association with tumor growth

Efterpi Dalpa[1] · Victor Gourvas[1] · Nikolaos Soulitzis[1] · Demetrios A. Spandidos[1]

Received: 7 October 2016 / Accepted: 22 November 2016 / Published online: 9 December 2016

Abstract Nephroblastoma (Wilms tumor) is a kidney neoplasia, predominately occurring at very young age, resulting from the malignant transformation of renal stem cells. The Ras proto-oncogenes and B-Raf are members of an intracellular cascade pathway, which regulates cell growth and differentiation, and ultimately cancer development. Our objective was to determine the mutation rate and to measure the mRNA levels of the three Ras genes and of B-Raf in formalin-fixed paraffin-embedded tissue samples from 32 patients with nephroblastoma and 10 controls. No mutations were detected in the four studied genes among our Wilms tumors cases, while Ras and B-Raf expression was higher in malignant samples versus controls. Statistical analysis revealed a positive correlation of K-Ras ($p < 0.001$) and B-Raf ($p = 0.006$) with tumor size, a negative correlation of K-Ras ($p = 0.041$) and H-Ras ($p = 0.033$) with the percentage of tissue necrosis, and an association of N-Ras ($p = 0.047$) and B-Raf ($p = 0.044$) with tissue histology. From the above, we deduce that although Ras and B-Raf mutations are rare events in Wilms tumors, their expression pattern suggests that they play an important role in the development and progression of this malignancy.

Keywords Nephroblastoma · RFLP · qPCR · Biomarkers · Oncogenes

✉ Demetrios A. Spandidos
spandidos@spandidos.gr

[1] Laboratory of Clinical Virology, Medical School, University of Crete, P.O. Box 2208, 71003 Heraklion, Crete, Greece

Introduction

Wilms tumor or nephroblastoma is the most common childhood malignancy of the abdomen. It affects 10 children per 1 million till the age of 15 and accounts for 7% of all childhood neoplasias, with median age at diagnosis 3.5 years. It is not gender specific (male to female ratio 0.95:1), although in bilateral cases the male to female ratio is 0.6:1 [1]. Imaging techniques and histological evaluation are crucial for the differential diagnosis of Wilms tumors from other childhood renal malignancies, such as mesoblastic nephroma, clear cell sarcoma, neuroblastoma, rhabdoid tumors and metanephric stromal tumors. Although nephroblastomas usually present the triphasic pattern of the normal kidney, consisting of cells with epithelial, blastemal, and stromal origin, in 3–7% of cases that have poorer survival, anaplastic elements are also detected [2]. Nephrogenic rests, dysplastic lesions of metanephric origin, which have been observed in 35% of nephroblastomas and probably represent precursor lesions, are linked with an increased risk of developing Wilms tumor, especially when found at a very young age and their location is perilobar [3]. Surgical removal of the tumor, accompanied by chemotherapy and/or radiotherapy is the usual treatment strategy. Survival rates, especially in the last decades, exceed 90% and only rare adult cases have worse prognosis [1].

Although nephroblastoma is considered a sporadic neoplasm, approximately 10% of cases are associated with congenital anomalies (WAGR, Denys-Drash, Frasier and Beckwith–Wiedemann syndromes, etc.) [4]. Several genetic alterations have been identified [5], such as mutations of the WT1 gene at chromosome 11p13, which was the first genetic modification to be associated with this tumor type [6]. Additional genetic loci that have been linked with nephroblastoma include 11p15 (WT2) [7],

Xq11.1 (WTX) [8], 17q12-q21 (FWT1) and 18q13.4 (FWT2) [9], 3p21 (CTNNB1) [10], 9q22.3 (PTCH1) [11] and 1p & 16q [12].

The Ras proto-oncogenes (K-Ras, H-Ras and N-Ras) encode for small GTPases that are members of the PI3K/AKT and MEK/ERK intracellular signaling pathways, which regulate cell growth and differentiation, and thus can play an important role in carcinogenesis [13, 14]. Indeed, Ras gene mutations have been detected in pancreatic, lung, colon and ovarian cancers (K-Ras), in bladder carcinomas (H-Ras), and in melanomas, lymphomas and thyroid malignancies (N-Ras). Codons 12, 13 and 61 are considered mutational "hot spots" [15, 16]. On the contrary, the mRNA expression of the three Ras oncogenes, especially in tumors that harbor no mutations, has been studied only in a few malignancies, such as bladder cancer [17], cervical carcinoma [18] and brain tumors [19].

B-Raf, a member of the Raf serine/threonine kinase family, is also a component of the MAPK signal transduction pathway, mediating cellular proliferation and migration, in response to various stimuli [20, 21]. Mutations in B-Raf lead to excessive cellular transformation and enhanced survival [22], and have been detected in 60–70% of malignant melanomas, in 35–55% of papillary thyroid tumors, in 5–20% of colorectal carcinomas, in ~30% of ovarian malignancies, and at lower rates in breast and lung neoplasms, sarcomas, gliomas, leukemias and lymphomas [23]. The most prominent mutation, accounting for 80–90% of all cases, is the T to A transversion at nucleotide 1799, which leads to the substitution of Valine (V) with Glutamate (E) at codon 600 (V600E) of the B-Raf protein [24]. Similarly to Ras, B-Raf mRNA expression has only been studied in thyroid carcinomas [25, 26].

Several reports have linked Wilms tumor 1 (WT1) [27–29] and β-Catenin (CTNNB1) [30] genes with the Ras signaling pathway and especially K-Ras, in a number of tissue cell lines, animal models and human neoplasms. Since WT1 and CTNNB1 mutations are crucial events in the development of nephroblastoma, one can hypothesize that the Ras/Raf pathway could also play a significant part during this tumorigenesis process. Therefore, we investigated the mutation rate, as well as the mRNA expression levels of the three Ras genes and of B-Raf, in tissue samples from Wilms tumors and controls, in order to elucidate their role in this renal malignancy.

Materials and methods

Study subjects

Formalin-fixed paraffin-embedded (FFPE) samples from 32 patients with Wilms tumors that underwent kidney surgery were obtained within a 3-year period at the "Ag. Sofia" General Children Hospital of Athens, Greece and at "G. Gennimatas" General Hospital of Thessaloniki, Greece. Samples from 10 cases that had their kidneys removed for non-neoplastic reasons (accidents, infections, etc.), served as the control group. All specimens were examined using hematoxylin and eosin-stained slides in order to verify the initial diagnosis. The clinical and histopathological characteristics of the study subjects are listed in Table 1. The Ethics Committees of the University of Crete, and of "Ag. Sofia" and "G. Gennimatas" Hospitals approved this study and written informed consent was obtained from all participants' legal guardians.

DNA extraction

DNA extraction was performed using the QIAamp® DNA FFPE Tissue Kit (Qiagen N.V., Venlo, Netherlands) according to the manufacturer's instructions. Briefly, five 10 μm thick sections from formalin fixed paraffin-embedded tissues were at first washed with xylene and then with absolute ethanol, in order to remove the paraffin. Samples were then incubated at 56 °C with Proteinase K, until the tissue completely dissolved, and then at 90 °C, in order to reverse DNA crosslink created by formaldehyde during the

Table 1 Clinical characteristics of the study groups

	Wilms tumors	Controls	*p* value
Cases (*n*)	32	10	
Age			
(mean ± SD, years)	3.1 ± 2.8	12.5 ± 7.5	**0.010**[a]
Gender			
Male (%)	15 (46.9)	5 (50.0)	1.00[b]
Female (%)	17 (53.1)	5 (50.0)	
Tumor location			
Left kidney (%)	15 (46.9)	6 (60.0)	0.47[b]
Right kidney (%)	17 (53.1)	4 (40.0)	
Maximum tumor diameter			
(mean ± SD, cm)	9.8 ± 4.1	–	–
Tumor origin			
Stromal (%)	43.0		
Epithelial (%)	30.0	–	–
Blastemal (%)	27.0		
Tissue necrosis			
(mean ± SD, %)	31.9 ± 14.8	–	–
Nephrogenic residues			
Yes (%)	13 (40.6)	–	–
No (%)	19 (59.4)		

Bold value indicates statistical significance

SD standard deviation

[a] Mann–Whitney *U* test (2-tailed)

[b] Chi-square or Fisher's exact test (2-tailed)

tissue fixation process. Subsequently, after a few washing steps, DNA was eluted in TE buffer and was stored at −20 °C until used.

PCR–RFLP analysis

The primers used for the identification of the codon 12 mutation hotspot of the three Ras genes, as well as the V600E mutation of the B-Raf gene, are listed in Table 2. PCR reactions were carried out at an annealing temperature of 58 °C (K-Ras, B-Raf) or 60 °C (H-Ras, N-Ras) and $MgCl_2$ concentration of 3 mM, using Pfu polymerase (Fermentas, Vilnius, Lithuania) for higher accuracy. 5 μl of each amplicon was run on 2% (w/v) agarose gels and stained with ethidium bromide in order to assess amplification.

PCR products (10 μl) were then incubated at 37 °C with 20 units of MvaI (K-Ras, N-Ras), MspI (H-Ras) and TspRI (B-Raf) endonucleases (Fermentas) for 16 h. Restriction fragments of each digestion reaction, which are exhibited in Table 2, were resolved on 2% (w/v) agarose gels and stained with ethidium bromide. All experimental procedures were carried out twice, and results were confirmed in representative samples by direct sequencing.

RNA extraction and cDNA preparation

RNA extraction was performed using the WaxFree™ FFPE RNA Extraction Kit (TrimGen Corp., Sparks, MD, USA) according to the manufacturer's protocol. RNA concentration and purity were calculated after measuring on a Nanodrop 1000 spectrophotometer (NanoDrop Products, Wilmington, DE) its 260 nm absorbance and 260/280 nm absorbance ratio, respectively.

cDNA was synthesized by reverse transcription (RT) with the RETROscript® Kit (Ambion Inc., Austin, TX, USA), using the Two Step RT-PCR Protocol. In detail, 2 μg of total RNA, 8.3 μM of random decamers and nuclease-free water up to a final volume of 12 μl were incubated for 3 min at 85 °C, in order to denaturate RNA secondary structures. Samples were immediately placed on ice for the addition of the remaining cDNA synthesis mix, which contained 10× RT Buffer (500 mM Tris–HCl, pH 8.3, 750 mM KCl, 30MmM $MgCl_2$, 50 mM DTT), 2.5 mM of each dNTP, 10units RNase Inhibitor and 100 units MMLV-RT Reverse Transcriptase. The final mix (total volume 20 μl) was incubated at 44 °C for 60 min for the reverse transcription reaction to take place, followed by incubation at 92 °C for 10 min to inactivate the reverse transcriptase. cDNA was stored at −20 °C until future use.

Quantitative real-time polymerase chain reaction (qPCR) assay

K-Ras, H-Ras, N-Ras and B-Raf mRNA expression was measured using a qPCR assay with the SYBR® Green I dye. The housekeeping gene, beta-actin (β-actin), was used as an internal control, in order to normalize the studied genes' expression levels. The mRNA-specific primers,

Table 2 Primers sequences used for PCR–RFLP and quantitative real-time PCR

Gene	Primer pair sequence (5′–3′)	Tm (°C)	PCR product (bp)	RFLP product (bp)
K-Ras	ACTGAATATAAACTTGTGGTAGTTGGACCT	58	157	Wt: 113 + 29 + 15
(DNA)	TCAAAGAATGGTCCTGGACC			Mut: 142 + 15
H-Ras	GAGACCCTGTAGGAGGACCC	60	312	Wt: 236 + 55 + 21
(DNA)	GGGTGCTGAGACGAGGGACT			Mut: 291 + 21
N-Ras	AACTGGTGGTGGTTGGACCA	60	83	Wt: 41 + 19 + 23
(DNA)	ATATTCATCTTACAAAGTGGTCCTGGA			Mut: 60 + 23
B-Raf	TCATAATGCTTGCTCTGATAGGA	58	224	Wt: 124 + 87 + 13
(DNA)	GGCCAAAAATTTAATCAGTGGA			Mut: 211 + 13
K-Ras	GGGGAGGGCTTTCTTTGTGTA	60	174	–
(RNA)	GTCCTGAGCCTGTTTTGTGTC			
H-Ras	GGGGCAGTCGCGCCTGTGAA	60	110	–
(RNA)	CCGGCGCCCACCACCACCAG			
N-Ras	GCCATCAATAATAGCAAG	55	86	–
(RNA)	ATAGGTACATCATCCGAGT			
B-Raf	GGGGCAGTCGCGCCTGTGAA	60	101	–
(RNA)	CCGGCGCCCACCACCACCAG			
β-actin	CGGCATCGTCACCAACTG	60	70	–
(RNA)	GGCACACGCAGCTCATTG			

which were designed with the Lasergene® software (DNASTAR, Madison, WI) and span at least one intron with an average length >800 bp, in order to avoid co-amplification of contaminating genomic DNA, are listed in Table 2. Their specificity was verified with the BLAST program (http://www.ncbi.nlm.nih.gov/BLAST). cDNA (1 μl) from Wilms tumors or controls was amplified in a PCR reaction (final volume 20 μl) containing 2× Maxima™ SYBR Green qPCR Master Mix (Fermentas) and 300 nM of each primer. After initial denaturation at 95 °C for 10 min, samples were subjected to 40 cycles of amplification, comprised of denaturation at 95 °C for 20 s, annealing at 60 °C (55 °C for N-Ras) for 30 s and elongation at 72 °C for 30 s, followed by a melt curve analysis, in which the temperature was increased from 60 to 95 °C at a linear rate of 0.2 °C/s. Data collection was performed during both annealing and extension, with two measurements at each step, and at all times during the melt curve analysis. To ensure the accuracy of the quantification measurements, a representative pool of all samples was diluted in a series of six 2× dilutions and was run on the same plate, in order to construct a standard curve for the quantification process. In each PCR reaction two negative controls were included, one with no cDNA template and one with no reverse transcription treatment. All qPCR experiments were conducted in triplicates and were run on an Mx3000P real-time PCR thermal cycler using software version 4.1 (Stratagene, La Jolla, CA, USA).

After amplification, standard curves were constructed from the samples used in the series of consecutive dilutions. Subsequently, using these standard curves and the Ct value of the "unknown" samples, we calculated the mRNA expression of the studied genes. Samples with no amplification plots or with dissociation curves that exhibited signs of primer-dimer formation or by-products were excluded. To normalize the mRNA expression of each gene, its value was divided by the same sample's β-actin mRNA value. The normalized values of Wilms tumors samples were divided by the average normalized values of control samples. The result of this division provided the relative expression of Wilms tumors specimens in relation to the control group. This mathematical process is summarized in the following formula:

$$\text{Normalized Sample/Control} = \left(1 + E_{\text{gene}}\right)^{-\Delta C_t\,\text{gene}} / \left(1 + E_{\beta-\text{actin}}\right)^{-\Delta C_t\,\beta-\text{actin}}$$

A twofold increased (a value ≥2) or decreased (a value ≤0.5) expression was considered biologically significant (overexpression or downregulation, respectively).

Ten microliters of PCR products was electrophorized on 2% (w/v) agarose gels and stained with ethidium bromide, in order to verify that the corresponding product band (as visualized with the help of a UV transilluminator) had the correct size. Representative bands of all PCR products were extracted from the agarose gels, purified and sequenced, as a final confirmation step that the appropriate gene was amplified in each PCR reaction.

Statistical analysis

K-Ras, H-Ras, N-Ras and B-Raf mRNA levels were first evaluated by the one sample Kolmogorov–Smirnov goodness-of-fit test, in order to determine whether they followed a normal distribution pattern. Depending on the results, Pearson's or the nonparametric Spearman's rank test was used, in order to examine their relationship pair-wise and their association with continuous variables (age, maximum tumor diameter, percentage of tissue necrosis). Moreover, their association with categorical data (gender, tumor kidney location, tumor cellular origin, the presence of nephrogenic residues) was determined by Student's t test (after examining for equality of variances with Levene's test), or by its nonparametric equivalents Mann–Whitney U and Kruskal–Wallis H tests. Additionally, the Chi-square (χ^2) test, replaced by Fisher's exact test when indicated by the analysis, was used to examine the studied genes' expression status in relation to the various clinicopathological parameters after stratification. Finally, univariate general linear model analysis, with age as cofactor, was used in order to correct the results for the age difference among the two study groups. Statistical analyses were two sided and were performed with the SPSS 11.5 software (SPSS, Chicago, IL, USA). Statistical significance was set at the 95% level (p value <0.05).

Results

Clinical data

Table 1 shows the clinicopathological characteristics of the two study groups. As was expected from the nature of this malignancy, subjects with Wilms tumors were significantly younger than controls (3.1 ± 2.8 vs. 12.5 ± 7.5 years, $p = 0.010$).

Mutation analysis

Our PCR–RFLP experiments did not reveal any mutations in the examined mutational hotspots of the three Ras genes and of B-Raf in our series of Wilms tumors, suggesting that these mutations are a rare event in this malignancy.

mRNA expression analysis

Our results revealed that all four studied genes had, on average, elevated mRNA levels in Wilms tumors compared with controls, with the average fold change ranging from 1.02 and 1.27 (for H-Ras and K-Ras, respectively) to 2.36 and 6.55 (for B-Raf and N-Ras, respectively) (Table 3; Fig. 1).

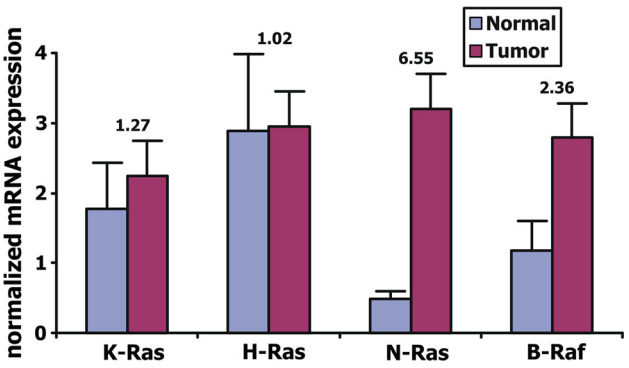

Fig. 1 *Bar chart* depicting K-Ras, H-Ras, N-Ras and B-Raf normalized mRNA expression in the control group and Wilms tumors, respectively. *Floating numbers* represent fold change between the two study groups

Statistical analysis

Statistical analysis revealed that K-Ras expression was higher in Wilms tumors with maximum tumor diameter larger than 10 cm when compared with tumor samples with maximum tumor diameter less than 10 cm (3.88 ± 1.16 vs. 0.73 ± 0.31, $p < 0.001$) (Fig. 2a), a finding that was also observed for B-Raf (4.21 ± 1.68 vs. 1.66 ± 0.65, $p = 0.006$) (Fig. 2b).

The statistical process also pointed out the correlation of H-Ras expression with the extent of tumor necrosis. Higher percentage of tissue necrosis was combined with lower H-Ras expression and vise versa (4.51 ± 0.61 vs. 2.34 ± 0.74, $p = 0.033$) (Fig. 2c). Additionally, higher tumor necrosis was associated with deregulated (elevated or reduced) K-Ras mRNA levels (K-Ras overexpression: $35.0 \pm 10.2\%$ tissue necrosis; K-Ras downregulation: $36.4 \pm 3.3\%$ tissue necrosis; K-Ras normal expression: $19.2 \pm 4.0\%$ tissue necrosis; $p = 0.041$) (Fig. 2d).

Finally, tumor histological features produced interesting statistically significant associations. N-Ras expression was higher when stromal and blastemal cells were the predominant tissue type, while its expression was lower when the tissue type was mainly of epithelial origin (Stromal: 4.16 ± 1.17; Blastemal: 1.64 ± 0.61, Epithelial: 0.79 ± 0.28, $p = 0.047$) (Fig. 2e). On the contrary, B-Raf expression was higher when epithelial and stromal cells were the predominant tissue type, while its expression was lower when blastemal elements were the majority of the tumor tissue (Epithelial: 3.76 ± 2.12, $p = 0.047$; Stromal: 3.43 ± 1.37; Blastemal: 0.92 ± 0.19; $p = 0.044$) (Fig. 2f). K-Ras and H-Ras expression did not differ among the various tumor tissue types.

Univariate analysis

In order to correct for the age discrepancy among the two study groups, we performed univariate general linear model analysis, with age as cofactor. Age-adjusted results did not differ statistically from the uncorrected ones (Table 3).

Co-expression analysis

Using Spearman's rank test, we tested the mRNA co-expression pattern of the four expressed genes in a pair-wise manner in both Wilms tumors and controls (after normalization). This test examines whether two molecules are upregulated or downregulated together (positive association), or whether when one is overexpressed the other has a reduced expression (negative association).

Table 3 mRNA expression analysis of K-Ras, H-Ras, N-Ras and B-Raf between Wilms tumors and controls

Gene	Wilms tumors	Controls	Fold change	P_c value*	P_a value§
K-Ras	2.25 ± 0.60	1.77 ± 0.67	1.27	0.69	0.11
H-Ras	2.95 ± 0.46	2.89 ± 1.09	1.02	0.96	0.26
N-Ras	3.20 ± 1.10	0.49 ± 0.11	6.55	0.21	0.39
B-Raf	2.79 ± 0.74	1.18 ± 0.42	2.36	0.30	0.11

All values are presented as mean ± SEM

* Student's *t* test

§ Univariate analysis using age as cofounding factor

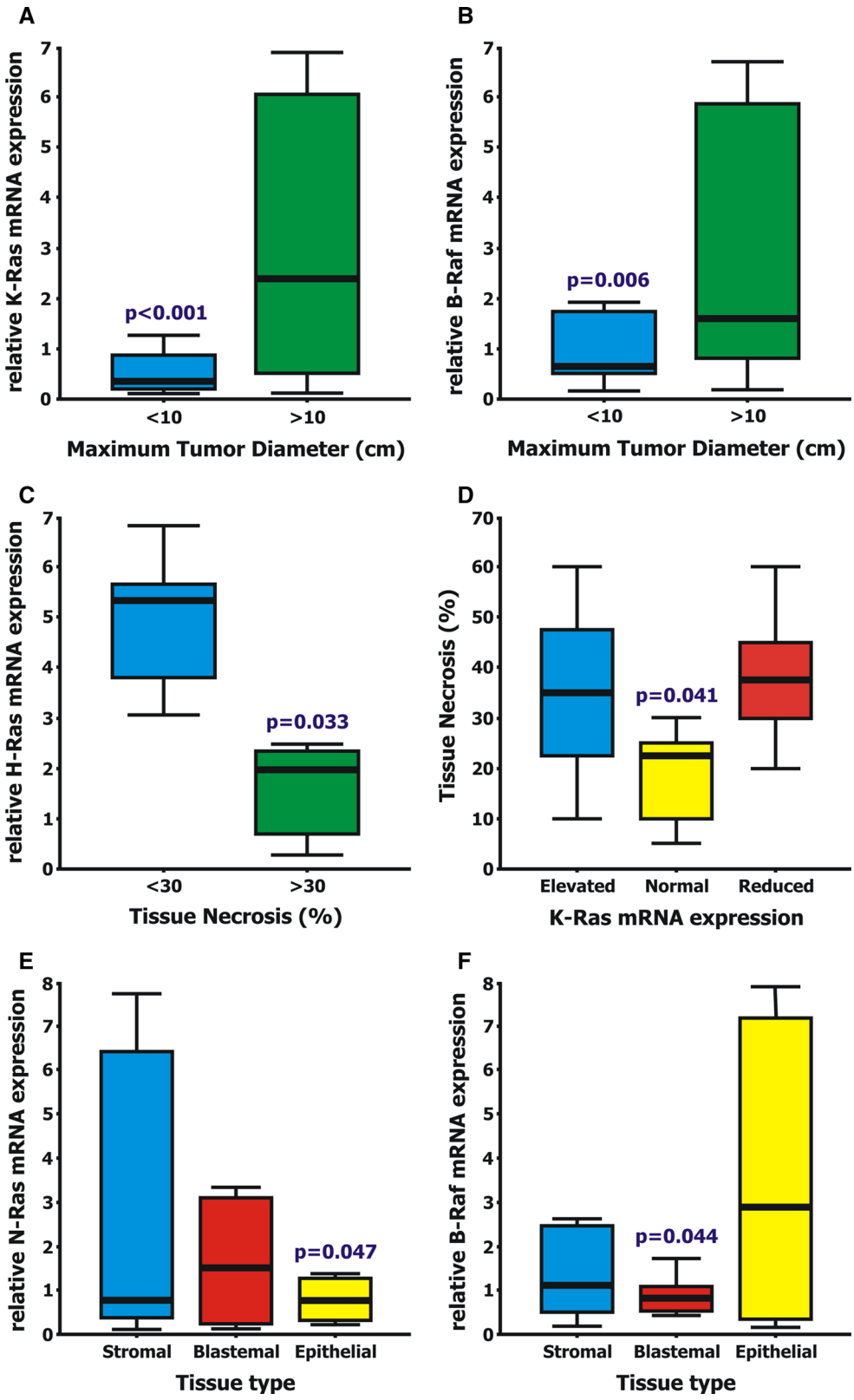
A
relative K-Ras mRNA expression
p<0.001
<10
>10
Maximum Tumor Diameter (cm)
B
relative B-Raf mRNA expression
p=0.006
<10
>10
Maximum Tumor Diameter (cm)
C
relative H-Ras mRNA expression
p=0.033
<30
>30
Tissue Necrosis (%)
D
Tissue Necrosis (%)
p=0.041
Elevated
Normal
Reduced
K-Ras mRNA expression
E
relative N-Ras mRNA expression
p=0.047
Stromal
Blastemal
Epithelial
Tissue type
F
relative B-Raf mRNA expression
p=0.044
Stromal
Blastemal
Epithelial
Tissue type

◀ **Fig. 2** *Box* and *whisker plots* depicting statistically significant associations. **a** K-Ras was upregulated in Wilms tumors with maximum tumor diameter (Max*D*) >10 cm versus tumors with Max*D* <10 cm (3.88 ± 1.16 vs. 0.73 ± 0.31, $p < 0.001$). **b** B-Raf was overexpressed in Wilms tumors with Max*D* >10 cm versus tumors with Max*D* <10 cm (4.21 ± 1.68 vs. 1.66 ± 0.65, $p = 0.006$). **c** H-Ras expression was higher in Wilms tumors with tissue necrosis <30% versus tumors with tissue necrosis >30% (4.51 ± 0.61 vs. 2.34 ± 0.74, $p = 0.033$). **d** Tissue necrosis was higher when K-Ras was either overexpressed (35.0 ± 10.2%) or downregulated (36.4 ± 3.3%), while it was lower when K-Ras expression was normal (19.2 ± 4.0%) ($p = 0.041$). **e** N-Ras expression was higher when stromal (4.16 ± 1.17) and blastemal (1.64 ± 0.61) cells were the predominant tumor tissue type, while its expression was lower when the tissue type was primarily of epithelial origin (0.79 ± 0.28) ($p = 0.047$). **f** B-Raf was overexpressed in epithelial (3.76 ± 2.12) and stromal (3.43 ± 1.37) tumor tissue types, while its expression was lower when blastemal elements predominated on the tumor tissue (0.92 ± 0.19) ($p = 0.044$). The *thick line* near the center of each *rectangular box* represents the median value, the *bottom* and *top edges* of the *box* indicate the 1st (Q_1) and 3rd (Q_3) quartiles, and the ends of the *whiskers* depict the 10th (P_{10}) and 90th (P_{90}) percentiles

In control samples, only K-Ras was positively associated with H-Ras ($p = 0.002$) (Table 4a). In Wilms tumors, we observed more (5 instead of 1) co-expressions between the studied genes than in controls. Specifically, the K-Ras—H-Ras association remained ($p = 0.006$), and in addition K-Ras was also co-expressed with N-Ras ($p < 0.001$) and B-Raf ($p < 0.001$). H-Ras was also positively correlated with B-Raf ($p < 0.001$) but not N-Ras ($p = 0.10$). Finally, N-Ras was co-expressed with B-Raf ($p = 0.001$) (Table 4b).

Table 4 Ras genes and B-Raf co-expression analysis in (A) controls and (B) Wilms tumors

	K-Ras	H-Ras	N-Ras	B-Raf
A. Controls				
K-Ras				
CC	1.000			
p value	–			
H-Ras				
CC	**0.905**	1.000		
p value	**0.002**	–		
N-Ras				
CC	−0.502	−0.180	1.000	
p value	0.17	0.67	–	
B-Raf				
CC	0.262	0.476	−0.048	1.000
p value	0.53	0.23	0.91	–
B. Wilms tumors				
K-Ras				
CC	1.000			
p value	–			
H-Ras				
CC	**0.498**	1.000		
p value	**0.006**	–		
N-Ras				
CC	**0.672**	0.314	1.000	
p value	**0.000**	0.10	–	
B-Raf				
CC	**0.786**	**0.617**	**0.539**	1.000
p value	**0.000**	**0.000**	**0.001**	–

Bold values indicate statistical significance

CC correlation coefficient

Discussion

The etiology of Wilms tumor has not been fully elucidated, although significant progress has been made regarding treatment strategies and increased survival rates. Several perinatal and environmental risk factors are considered to play a significant role in this malignancy, such as smoking and exposure to chemicals, high birth weight, preterm birth, maternal hypertension and being first born [31, 32]. The presence of nephrogenic rests is also linked to increased risk of developing nephroblastoma. They are divided into two groups depending on their location within the kidney, named intralobar (ILNR) or perilobar (PLNR) nephrogenic rests, respectively. ILNRs are linked to syndromes associated with WT1 gene mutations or deletions, such as WAGR and Denys–Drash syndromes, while PLNRs are more frequent and are mostly related to overgrowth irregularities, such as Beckwith-Wiedemann syndrome and hemihypertrophy, which are linked to the loss of IGF2 imprinting [33, 34]. Mutations of the WT1, CTNNB1 and WTX genes are also important, although they only occur in approximately one third of Wilms tumors cases [7, 10, 35, 36]. Epigenetic events are also crucial for the development of nephroblastoma, occurring predominately at the WT2 locus (11p15.5) and involve H19 hypermethylation and loss of IGF2 imprinting [37–39]. This accumulated data have let scientists to propose two distinct models/mechanisms regarding the development/pathogenesis of Wilms tumors. The first one is characterized by later age of onset, high birth weight, overgrowth syndromes, the presence of PLNRs and of anaplastic or blastemal/epithelial histological elements, and of IGF2 loss of imprinting. The second one is associated with earlier disease onset, abnormalities in the genitourinary tract, the presence of ILNRs and stromal histological elements, and of WT1 gene mutations [31, 32, 34].

Since Ras and B-Raf are among the most common genes associated with neoplasmatic diseases and are mainly activated through point mutations, we investigated for possible mutations at their mutational hotspots in our nephroblastoma cases. None of the 32 Wilms tumor

specimens harbored any of the examined mutations among the four studied genes. These findings are in compliance with previous, although very limited in number, reports about the occurrence of Ras [40, 41] and B-Raf [42] mutations in nephroblastomas.

However, the presence of wild-type Ras and Raf genes does not rule out the participation of the Ras/Raf/Mek/Erk pathway in the pathogenesis of nephroblastoma, especially since members of the Ras pathway have been linked to CTNNB1-mutated Wilms tumors [43]. Therefore, we also evaluated the mRNA expression of K-Ras, H-Ras, N-Ras and B-Raf genes in our Wilms tumors, using the control group in order to determine the expression of the studied genes under normal conditions. Our results showed that the three Ras genes and B-Raf were deregulated in Wilms tumors versus controls. This is the first study to measure the mRNA expression of the Ras genes in Wilms tumors. There have been only two contradictory reports regarding the expression of the Ras p21 protein in childhood renal tumors, with one finding p21 overexpression in tumor samples versus pre-malignant or benign legions and normal kidneys [44], while the other failed to find a significant staining presence of p21 within cancer specimens [45]. As for B-Raf, no data exist regarding its mRNA or protein levels in nephroblastomas or other related neoplasias.

Statistical analysis revealed several interesting associations between the studied molecules mRNA expression and various tumor histological parameters. Initially, a positive correlation among K-Ras and B-Raf expression and increasing tumor diameter was established ($p < 0.001$ and $p = 0.006$, respectively). Previous studies have suggested an association of VEGF [46], matrix-metalloproteinase-4 (MMP4) [47] and Her2/neu (ERBB2) [48] with tumor growth in nephroblastoma, since inhibiting these molecules resulted in tumor growth arrest. Additionally, K-Ras has been associated with tumor growth in pancreatic cancer [49], malignant mesothelioma [50], hepatocellular carcinoma [51], nasopharyngeal tumors [52] and non-small cell lung cancer [53], while B-Raf has been linked with increased tumor proliferation in malignant melanoma [54] and thyroid cancer [55].

Another interesting statistically significant association was the reduced mRNA levels of H-Ras and the deregulation of K-Ras expression in malignant cases with extended tissue necrosis ($p = 0.033$ and $p = 0.041$, respectively). Large percent of tissue necrosis is associated with rapid tumor expansion, as has been demonstrated in immortalized fibroblasts that contain activated H-Ras through mutations [56, 57], and has been linked to poor prognosis. However, recent reports suggest that wild-type Ras genes induce apoptosis and have an onco-suppressive role, in contrast to the oncogenic potential of the mutated ones [58, 59]. Therefore, in our Wilms tumor cases, cancer cells probably decrease wild-type H-Ras expression and promote tumor proliferation via alternative pathways, which ultimately leads to increased tissue necrosis [60]. The same logic can be applied to the percentage of tumors that downregulated K-Ras. As for those malignancies, in which K-Ras was upregulated, its protective effect is probably negated by the activation of other anti-apoptotic or cell proliferation pathways [61, 62].

Finally, significant correlations with tumor histology were observed. N-Ras mRNA levels were higher in tumors with predominately stromal tissue origin and lower in tumors with predominately epithelial origin ($p = 0.047$), while B-Raf expression was elevated in neoplasias with either epithelial or stromal origin and reduced in neoplasias with blastemal tissue origin ($p = 0.044$). The prevalence of epithelial elements within the tumor tissue, in contrast to blastemal ones, leads to better disease prognosis, suggesting a protective role for wild-type B-Raf in epithelial cells. On the contrary, with its downregulation, wild-type N-Ras loses its anti-oncogenic potential [63, 64].

One significant limitation of this study is the relative low number of Wilms tumor cases and controls. Although the exact incident rate of Wilms tumors in our country is unknown, based on the American estimate of 500 cases per year (in a population of 320 million people vs. 11 million in Greece), and taking into account the lower birth rates per 1.000 people in Greece (8.66 vs. 12.49), approximately 10–20 (median 15) nephroblastoma cases per year occur in our country. Therefore, it would take an even longer amount of time to gather more samples, that the 3 years it took us to gather our 32 cases. The same applies to the control group, since we wanted our controls to have normal kidney histology and function. Therefore, we could not recruit children with other renal malignancies as controls, but only otherwise healthy children that had their kidney removed due to trauma or infection.

Another limitation of the study is the age discrepancy between our two study groups, since by the nature of this type of malignancy, the median age among our Wilms tumors patients was approximately 3 years old. Additionally, due to the rarity of the controls, and in order to find a sufficient number for our research, we had to be less strict regarding the age criteria, resulting in a median age of 12.5 years. Fortunately, we were able to overcome this shortcoming, by performing a univariate analysis in our crude Ras and B-Raf mRNA levels, correcting for this age discrepancy among the two groups. Interestingly, our studied genes expression results did not change their significance, once corrected for age.

Finally, due to the chemical procedure that takes place during tissue preservation (formaldehyde cross-linking), nucleic acids are severely modified and degraded, and continue to do so, the longer the paraffin blocks are stored.

Therefore, the quality of the extracted RNA, which itself is a much more sensitive nucleic acid than DNA, is not optimal, potentially leading to false expression data. However, the recently developed extraction methods, such as the one we used, ensure that the damage that RNA has sustained would be minimal. Additionally, the fact that the origin of both study groups specimens were from FFPE tissues means that RNA was equally degraded in all cases. Finally, the fact that our cDNA amplicons had small sizes (<200 bp), ensures their proper amplification, since during primer design we took into account the information that the length of the extracted RNA from FFPE tissues is usually <500 bp.

Conclusion

Despite the lack of mutations, our expression data suggest that the Ras/Raf pathway plays a significant role in the development and progression of nephroblastoma. Since they may have a more diverse role than initially believed, new in-depth studies are needed in order to clarify the role of each gene and their encoded proteins in Wilms tumors, and to decipher the molecular mechanisms that lead to this pediatric neoplasm, paving the way to a possible treatment in the future.

Compliance with ethical standards

Conflict of interest The authors have no conflicts of interest to declare.

Ethical approval All procedures performed in our study involving human participants were in accordance with the ethical standards of the Research Committees of the University of Crete, and of "Ag. Sofia" and "G. Gennimatas" Hospitals, and with the 1964 Helsinki Declaration and its later amendments.

Informed consent Written informed consent was obtained from the legal guardians of all individual participants included in the study.

References

1. Breslow N, Olshan A, Beckwith JB, Green DM. Epidemiology of Wilms tumor. Med Pediatr Oncol. 1993;21:172–81.
2. van den Heuvel-Eibrink MM, Grundy P, Graf N, Pritchard-Jones K, Bergeron C, Patte C, et al. Characteristics and survival of 750 children diagnosed with a renal tumor in the first seven months of life: a collaborative study by the SIOP/GPOH/SFOP, NWTSG, and UKCCSG Wilms Tumor Study Groups. Pediatr Blood Cancer. 2008;50:1130–4.
3. Coppes MJ, Arnold M, Beckwith JB, Ritchey ML, D'Angio GJ, Green DM, et al. Factors affecting the risk of contralateral Wilms tumor development: a report from the National Wilms Tumor Study Group. Cancer. 1999;85:1616–25.
4. Scott RH, Stiller CA, Walker L, Rahman N. Syndromes and constitutional chromosomal abnormalities associated with Wilms tumour. J Med Genet. 2006;43:705–15.
5. Coppes MJ, Haber DA, Grundy PE. Genetic events in the development of Wilms' tumor. N Engl J Med. 1994;331:586–90.
6. Knudson AG Jr, Strong LC. Mutation and cancer: a model for Wilms' tumor of the kidney. J Natl Cancer Inst. 1972;48:313–24.
7. Satoh Y, Nakadate H, Nakagawachi T, Higashimoto K, Joh K, Masaki Z, et al. Genetic and epigenetic alterations on the short arm of chromosome 11 are involved in a majority of sporadic Wilms' tumours. Br J Cancer. 2006;95:541–7.
8. Rivera MN, Kim WJ, Wells J, Driscoll DR, Brannigan BW, Han M, et al. An X chromosome gene, WTX, is commonly inactivated in Wilms tumor. Science. 2007;315:642–5.
9. Ruteshouser EC, Huff V. Familial Wilms tumor. Am J Med Genet C Semin Med Genet. 2004;129C:29–34.
10. Koesters R, Ridder R, Kopp-Schneider A, Betts D, Adams V, Niggli F, et al. Mutational activation of the beta-catenin proto-oncogene is a common event in the development of Wilms' tumors. Cancer Res. 1999;59:3880–2.
11. Isidor B, Bourdeaut F, Lafon D, Plessis G, Lacaze E, Kannengiesser C, et al. Wilms' tumor in patients with 9q22.3 microdeletion syndrome suggests a role for PTCH1 in nephroblastomas. Eur J Hum Genet. 2013;21:784–7.
12. Grundy PE, Breslow NE, Li S, Perlman E, Beckwith JB, Ritchey ML, et al. Loss of heterozygosity for chromosomes 1p and 16q is an adverse prognostic factor in favorable-histology Wilms tumor: a report from the National Wilms Tumor Study Group. J Clin Oncol. 2005;23:7312–21.
13. Barbacid M. Ras genes. Annu Rev Biochem. 1987;56:779–827.
14. Grand RJ, Owen D. The biochemistry of ras p21. Biochem J. 1991;279(Pt 3):609–31.
15. Kiaris H, Spandidos D. Mutations of ras genes in human tumors (review). Int J Oncol. 1995;7:413–21.
16. Karnoub AE, Weinberg RA. Ras oncogenes: split personalities. Nat Rev Mol Cell Biol. 2008;9:517–31.
17. Vageli D, Kiaris H, Delakas D, Anezinis P, Cranidis A, Spandidos DA. Transcriptional activation of H-ras, K-ras and N-ras proto-oncogenes in human bladder tumors. Cancer Lett. 1996;107:241–7.
18. Mammas IN, Zafiropoulos A, Koumantakis E, Sifakis S, Spandidos DA. Transcriptional activation of H- and N-ras oncogenes in human cervical cancer. Gynecol Oncol. 2004;92:941–8.
19. Lymbouridou R, Soufla G, Chatzinikola AM, Vakis A, Spandidos DA. Down-regulation of K-ras and H-ras in human brain gliomas. Eur J Cancer. 2009;45:1294–303.
20. Marais R, Marshall CJ. Control of the ERK MAP kinase cascade by Ras and Raf. Cancer Surv. 1996;27:101–25.
21. Robinson MJ, Cobb MH. Mitogen-activated protein kinase pathways. Curr Opin Cell Biol. 1997;9:180–6.
22. Wan PT, Garnett MJ, Roe SM, Lee S, Niculescu-Duvaz D, Good VM, et al. Mechanism of activation of the RAF-ERK signaling pathway by oncogenic mutations of B-RAF. Cell. 2004;116:855–67.
23. Garnett MJ, Marais R. Guilty as charged: B-RAF is a human oncogene. Cancer Cell. 2004;6:313–9.
24. Davies H, Bignell GR, Cox C, Stephens P, Edkins S, Clegg S, et al. Mutations of the BRAF gene in human cancer. Nature. 2002;417:949–54.
25. Araujo PP, Marcello MA, Tincani AJ, Guilhen AC, Morari EC, Ward LS. mRNA BRAF expression helps to identify papillary thyroid carcinomas in thyroid nodules independently of the presence of BRAFV600E mutation. Pathol Res Pract. 2012;208:489–92.
26. Derdas SP, Soulitzis N, Balis V, Sakorafas GH, Spandidos DA. Expression analysis of B-Raf oncogene in V600E-negative benign and malignant tumors of the thyroid gland: correlation with late disease onset. Med Oncol. 2013;30:336.

27. Luo XN, Reddy JC, Yeyati PL, Idris AH, Hosono S, Haber DA, et al. The tumor suppressor gene WT1 inhibits ras-mediated transformation. Oncogene. 1995;11:743–50.
28. Vicent S, Chen R, Sayles LC, Lin C, Walker RG, Gillespie AK, et al. Wilms tumor 1 (WT1) regulates KRAS-driven oncogenesis and senescence in mouse and human models. J Clin Invest. 2010;120:3940–52.
29. Wu C, Wang S, Xu C, Tyler A, Li X, Andersson C, et al. WT1 enhances proliferation and impedes apoptosis in KRAS mutant NSCLC via targeting cMyc. Cell Physiol Biochem. 2015;35: 647–62.
30. Clark PE, Polosukhina D, Love H, Correa H, Coffin C, Perlman EJ, et al. beta-Catenin and K-RAS synergize to form primitive renal epithelial tumors with features of epithelial Wilms' tumors. Am J Pathol. 2011;179:3045–55.
31. Breslow NE, Beckwith JB, Perlman EJ, Reeve AE. Age distributions, birth weights, nephrogenic rests, and heterogeneity in the pathogenesis of Wilms tumor. Pediatr Blood Cancer. 2006;47: 260–7.
32. Chu A, Heck JE, Ribeiro KB, Brennan P, Boffetta P, Buffler P, et al. Wilms' tumour: a systematic review of risk factors and meta-analysis. Paediatr Perinat Epidemiol. 2010;24:449–69.
33. Beckwith JB. Nephrogenic rests and the pathogenesis of Wilms tumor: developmental and clinical considerations. Am J Med Genet. 1998;79:268–73.
34. Fukuzawa R, Reeve AE. Molecular pathology and epidemiology of nephrogenic rests and Wilms tumors. J Pediatr Hematol Oncol. 2007;29:589–94.
35. Huff V. Wilms tumor genetics. Am J Med Genet. 1998;79:260–7.
36. Ruteshouser EC, Robinson SM, Huff V. Wilms tumor genetics: mutations in WT1, WTX, and CTNNB1 account for only about one-third of tumors. Genes Chromosom Cancer. 2008;47:461–70.
37. Moulton T, Crenshaw T, Hao Y, Moosikasuwan J, Lin N, Dembitzer F, et al. Epigenetic lesions at the H19 locus in Wilms' tumour patients. Nat Genet. 1994;7:440–7.
38. Steenman MJ, Rainier S, Dobry CJ, Grundy P, Horon IL, Feinberg AP. Loss of imprinting of IGF2 is linked to reduced expression and abnormal methylation of H19 in Wilms' tumour. Nat Genet. 1994;7:433–9.
39. Ravenel JD, Broman KW, Perlman EJ, Niemitz EL, Jayawardena TM, Bell DW, et al. Loss of imprinting of insulin-like growth factor-II (IGF2) gene in distinguishing specific biologic subtypes of Wilms tumor. J Natl Cancer Inst. 2001;93:1698–703.
40. Baird P, Wadey R, Cowell J. Loss of heterozygosity for chromosome region 11p15 in Wilms' tumours is not related to HRAS gene transforming mutations. Oncogene. 1991;6:1147–9.
41. Waber PG, Chen J, Nisen PD. Infrequency of ras, p53, WT1, or RB gene alterations in Wilms tumors. Cancer. 1993;72:3732–8.
42. Miao J, Kusafuka T, Fukuzawa M. Hotspot mutations of BRAF gene are not associated with pediatric solid neoplasms. Oncol Rep. 2004;12:1269–72.
43. Zirn B, Samans B, Wittmann S, Pietsch T, Leuschner I, Graf N, et al. Target genes of the WNT/beta-catenin pathway in Wilms tumors. Genes Chromosom Cancer. 2006;45:565–74.
44. Kumar S, Hand PH, Marsden HB, Kumar P, Thor A. Quantitation of enhanced expression of ras-oncogene product (p21) in childhood renal tumours. Anticancer Res. 1991;11:1657–62.
45. Aoki I, Yanoma S, Misugi K, Sasaki Y, Kikyo S. Ras p21 expression in nephroblastoma group tumors. Acta Pathol Jpn. 1987;37:1903–7.
46. Rowe DH, Huang J, Kayton ML, Thompson R, Troxel A, O'Toole KM, et al. Anti-VEGF antibody suppresses primary tumor growth and metastasis in an experimental model of Wilms' tumor. J Pediatr Surg. 2000;35:30–2.
47. Celiker MY, Wang M, Atsidaftos E, Liu X, Liu YE, Jiang Y, et al. Inhibition of Wilms' tumor growth by intramuscular administration of tissue inhibitor of metalloproteinases-4 plasmid DNA. Oncogene. 2001;20:4337–43.
48. Yokoi A, McCrudden KW, Huang J, Kim ES, Soffer SZ, Frischer JS, et al. Human epidermal growth factor receptor signaling contributes to tumor growth via angiogenesis in her2/neu-expressing experimental Wilms' tumor. J Pediatr Surg. 2003;38:1569–73.
49. Mackenzie GG, Bartels LE, Xie G, Papayannis I, Alston N, Vrankova K, et al. A novel Ras inhibitor (MDC-1016) reduces human pancreatic tumor growth in mice. Neoplasia. 2013;15: 1184–95.
50. Khodayari N, Mohammed KA, Goldberg EP, Nasreen N. EphrinA1 inhibits malignant mesothelioma tumor growth via let-7 microRNA-mediated repression of the RAS oncogene. Cancer Gene Ther. 2011;18:806–16.
51. Charette N, De Saeger C, Lannoy V, Horsmans Y, Leclercq I, Starkel P. Salirasib inhibits the growth of hepatocarcinoma cell lines in vitro and tumor growth in vivo through ras and mTOR inhibition. Mol Cancer. 2010;9:256.
52. Deng M, Tang H, Zhou Y, Zhou M, Xiong W, Zheng Y, et al. miR-216b suppresses tumor growth and invasion by targeting KRAS in nasopharyngeal carcinoma. J Cell Sci. 2011;124: 2997–3005.
53. Sunaga N, Shames DS, Girard L, Peyton M, Larsen JE, Imai H, et al. Knockdown of oncogenic KRAS in non-small cell lung cancers suppresses tumor growth and sensitizes tumor cells to targeted therapy. Mol Cancer Ther. 2011;10:336–46.
54. Hoeflich KP, Gray DC, Eby MT, Tien JY, Wong L, Bower J, et al. Oncogenic BRAF is required for tumor growth and maintenance in melanoma models. Cancer Res. 2006;66:999–1006.
55. Chiappetta G, Basile A, Arra C, Califano D, Pasquinelli R, Barbieri A, et al. BAG3 down-modulation reduces anaplastic thyroid tumor growth by enhancing proteasome-mediated degradation of BRAF protein. J Clin Endocrinol Metab. 2012;97:E115–20.
56. Peretz D, Kimel N, Fujii DK, Neufeld G. Overexpression of basic fibroblast growth factor complementary DNA in Ha-ras-transformed cells correlates with a decreased incidence of tumor necrosis. Cancer Res. 1993;53:158–64.
57. Arends MJ, McGregor AH, Wyllie AH. Apoptosis is inversely related to necrosis and determines net growth in tumors bearing constitutively expressed myc, ras, and HPV oncogenes. Am J Pathol. 1994;144:1045–57.
58. Spandidos DA, Sourvinos G, Tsatsanis C, Zafiropoulos A. Normal ras genes: their onco-suppressor and pro-apoptotic functions (review). Int J Oncol. 2002;21:237–41.
59. Singh A, Sowjanya AP, Ramakrishna G. The wild-type Ras: road ahead. FASEB J. 2005;19:161–9.
60. Grabocka E, Pylayeva-Gupta Y, Jones MJ, Lubkov V, Yemanaberhan E, Taylor L, et al. Wild-type H- and N-Ras promote mutant K-Ras-driven tumorigenesis by modulating the DNA damage response. Cancer Cell. 2014;25:243–56.
61. Zhang Z, Wang Y, Vikis HG, Johnson L, Liu G, Li J, et al. Wildtype Kras2 can inhibit lung carcinogenesis in mice. Nat Genet. 2001;29:25–33.
62. Luo F, Poulogiannis G, Ye H, Hamoudi R, Dong G, Zhang W, et al. Wild-type K-ras has a tumour suppressor effect on carcinogen-induced murine colorectal adenoma formation. Int J Exp Pathol. 2014;95:8–15.
63. Benet M, Dulman RY, Suzme R, de Miera EV, Vega ME, Nguyen T, et al. Wild type N-ras displays anti-malignant properties, in part by downregulating decorin. J Cell Physiol. 2012;227:2341–51.
64. Mar VJ, Wong SQ, Li J, Scolyer RA, McLean C, Papenfuss AT, et al. BRAF/NRAS wild-type melanomas have a high mutation load correlating with histologic and molecular signatures of UV damage. Clin Cancer Res. 2013;19:4589–98.